Int. J. Electrochem. Sci., 7 **(2012)** 6106 - 6117

International Journal of
ELECTROCHEMICAL
SCIENCE
www.electrochemsci.org

Evaluation of ZrO_2 Composite Membrane Operating at High Temperature (100 °C) in Direct Methanol Fuel Cells.

C. Guzmán[1,4], *A. Alvarez*[2], *Luis A. Godínez*[3], *J. Ledesma–García*[1,*], *L. G. Arriaga*[3,*]

[1] División de Investigación y Posgrado, Facultad de Ingeniería, Universidad Autónoma de Querétaro, C.P. 76010, Querétaro, México.
[2] División Académica, Universidad Tecnológica de Corregidora, C.P. 76900 Querétaro, México.
[3] Centro de Investigación y Desarrollo Tecnológico en Electroquímica S.C., C.P. 76703, Querétaro, México.
[4] UACQ – UAZ, CU Siglo XXI Edificio b, Km 6 Carr. Zac – Gdl, La Escondida Zacatecas, Zac, C.P. 96160, México.
[*]E-mail: janet.ledesma@uaq.mx; larriaga@cideteq.mx

Received: 23 April 2012 / *Accepted:* 5 June 2012 / *Published:* 1 July 2012

This study focuses on the effect of two different membranes, a Zirconium Dioxide composite membrane versus a commercial membrane (Nafion – 112) on the performance of a methanol fuel cell at high temperatures (100 ºC) . The inorganic material was synthesized using the sol gel method. Then, the inorganic filler was mixed with a Nafion (5%) solution and dried in order to obtain the composite membrane. This composite material was characterized by SEM and FTIR, thus confirming the inclusion of the inorganic oxide into the Nafion matrix. Ion exchange capacity and water uptake values were obtained from the membranes observing that the composite membrane should show a similar behavior than that of the Nafion membrane. From the fuel cell tests, it was observed that the composite zirconium membrane has better performance than that obtained from the commercial membrane. This difference was related to the influence of the inorganic modifier in partial suppression of the methanol crossover effect.

Keywords: High temperature methanol fuel cells, composite membrane

1. INTRODUCTION

Direct Methanol Fuel Cells (DMFC's) constitute a suitable technology for portable electronic devices and vehicle related applications, due to their intrinsic requirement of to a liquid fuel with relatively high power density and its easy storage and handling [1-3]. For these devices, Nafion is still

the most common membrane due to its high proton conductivity and its chemical and electrochemical stability. However, the use of this membrane leads to a significant decrease in the fuel cell performance due to the methanol crossover effect [4-6]. Methanol crossover not only lowers the fuel availability, but also the reduction of active sites on the cathode that results in lower levels of performance [7]. In recent years significant research efforts have focused on the development of new membranes to reduce the methanol crossover [8-11] and to allow higher operating temperatures (> 100 °C) [12-15]. DMFC operation at elevated temperature improves the tolerance to CO contamination [16], enhancing the kinetics of both electrodes [13] and facilitating heat removal [17, 18].

One approach to improve the Nafion membrane properties in this direction consists on mixing liquid Nafion with inorganic compounds such as TiO_2, ZrO_2 and SiO_2 [13, 16, 19]. The presence of the inorganic fillers in the Nafion matrix enhances water retention at high temperatures [15] and reduces the methanol crossover effect [13]. The aim of the present work is to evaluate the influence of a composite membrane based on ZrO_2 in a DMFC operating at high temperature (100 °C) and compare the results to those obtained using a commercial Nafion 115 membrane.

2. EXPERIMENTAL

2.1 Synthesis of ZrO_2

ZrO_2 was prepared using the sol–gel technique utilizing zirconium (IV) propoxide, (70 wt %, Aldrich) as a precursor and aqueous HNO_3 with a 1:1 molar ratio as a catalyst. This colloidal solution was kept at room temperature until solid formation [20-26]. The resulting solid was thermally treated using a tubular furnace (Barnstead Thermolyne) at 150°C for 2 hrs in order to remove the residual alcohol.

2.2 Preparation of the composite membrane

A 5% (w/w) Ion Power Nafion alcoholic solution (LQ1105) was selected to manufacture the film. The original solution was dried at T=40°C, and subsequently diluted with dimethylacetammide (DMAc) in order to obtain a 20% (w/w) solution. This solution was used to cast, by the Doctor-Blade method, a membrane. For each composite membrane, a mixture of 3% (w/w) of the oxide powder and 97% (w/w) of the dry Nafion resin was added. For each composite membrane, an amount of 3% (w/w) of oxide powder compared to the dry Nafion resin was added to 20% (w/w) polymeric solution and dispersed in an ultrasonic bath for 30 min before the re-concentration phase necessary for the casting procedure. Through a slow re-concentration at 80°C under magnetic stirring, suitable viscosity solutions were obtained and stratified on a glass sheet. The obtained membranes were dried on a hot plate at T=80°C for 3hrs to evaporate the solvent and, then, detached from the glass with distilled water. The membranes thus prepared underwent a thermal treatment (T=155°C for 30 minutes) to favor the crystalline phase of the polymer and to improve the mechanical properties. Later, a chemical treatment using HNO_3 at 80°C for 30 minutes was carried out. Finally a boiling step in distilled water

was also employed (15 minutes) and a treatment in a 1M H_2SO_4 solution at 80°C for 30 minutes was employed [27-29].

2.3 Composite Membrane Characterization

2.3.1 Physicochemical methods

Fourier transform infrared (FT-IR) spectra were collected using a Bruker (Vector 33). While the spectral range of 400 to 4000 cm-1 was employed in the transmission mode. The morphology of the composite membrane on the other hand, was examined using a Scanning Electron Microscope (SEM) Jeol model JSM-5400 LV with a 15 keV voltage acceleration value.

2.3.2 Ionic exchange capacity (IEC)

The *IEC* of the membranes was determined through an acid-base titration with an automatic titrator (Metrohm, mod. 751 GPD Titrino). In these experiments, the membranes were first dried at 80°C for 2h in an oven under vacuum to determine the dried weight. Then, they were immersed in a 1 M NaCl solution to exchange the H^+ ions of the SO_3H group by Na^+ cations and the resulting solution was titrated using a 10^{-2} M NaOH solution to neutralize the exchanged H+. Using the equivalent point obtained from the plot of the pH value vs the added titrant volume and the dry weight of each sample, the *IEC* of the membrane can be calculated using the following relation:

$$IEC = \frac{(V*M)}{m_{dry}} \qquad [1]$$

where *IEC* is the ionic exchange capacity in SO_3H meq g^{-1}; *V*, is the added titrant volume at the equivalent point in ml; *M*, is the molar concentration of the titrant, and m_{dry} is the dry mass of the sample in g [30].

2.3.3 Water Uptake (W_{up})

The water uptake (Wup, %) was determined from the difference between the wet and the dry mass of the membrane. While the dry mass was obtained from the vacuum oven dried samples (at 80°C for 2 h), the wet mass was determined from distilled H_2O swelled samples (24 h) prepared at room temperature. [27-29]. The corresponding equation for W_{up} determnation is:

$$W_{up} = \left[M_{wet} - \frac{M_{dry}}{M_{wet}}\right] * 100 \qquad [2]$$

Where:

M_{wet} and M_{dry} correspond to the wet and dry weights, respectively.

On the other hand, Eq. (3) was used to determine the number of water molecules per sulfonated group (λ). In this equation, 18 is the molar mass of water and the IEC value employed corresponds to that obtained from [31].

$$\lambda = \frac{H_2O}{SO_3^-} = \left(\frac{Water\ Uptake}{18 * IEC}\right) * (10) \qquad [3]$$

2.4 Electrochemical characterization

2.4.1 Measurement of methanol permeability.

A two-compartment glass cell (3.4 mL) was used to investigate the methanol permeability of the membranes at 25 C. In this way, while compartment I was filled with an aqueous solution containing 1 M methanol and 0.5M H_2SO_4; compartment II was filled with the same amount of O.5M H_2SO_4 solution than that in compartment I. The membrane was clamped between the two compartments, and the two solutions were continuously stirred during the experiments. The methanol concentration in compartment II was monitored by chronoamperometry [32]. In this way, a constant potential 0.679V vs Ag/AgCl was applied for 240 s, using a BAS-Epsilon potentiostat (EC EPSILON). In these experiments, a Pt micro electrode served as working electrode (WE), and a Ag/AgCl and Pt wire were a reference and a counter electrode (CE), respectively. From the permeated methanol concentration value at any time it is possible to estimate the methanol permeability (P) using equation (4):

$$C_{II} = \frac{A}{V_{II}} \frac{DK}{L} C_I t \qquad [4]$$

Where C_{II} is the methanol concentration in compartment II, C_I is the methanol concentration in compartment I, A and L are the area and thickness of the membrane, D and K are the methanol diffusivity and the partition coefficient between the membrane and the adjacent solution, *t* is the permeation time, and V_{II} is the volume of the solution in compartment II. The product DK is the methanol permeability P.

2.5 Fuel cell performance tests

Fuel cell performance tests were carried out using a commercial 5 cm^2 fuel cell device (Electrochem) arranged with the Nafion and the composite membranes. The electrodes were home made using 4 mg cm^{-2} of Pt – Ru (60 %) for the anode and 1 mg cm^{-2} of Pt – C (30%) for the cathode. [ref] Carbon cloths were used to construct the diffusion layer. The direct methanol fuel cell was operated with 2M of MeOH (aq) at a fixed flow rate of 8 mL and oxygen fully humidified at a fixed flow rate of 200 mL min^{-1}. The back pressure was 30 psi in both electrodes. The fuel cell measurements were made using a Compucell fuel cell test system. The temperature of the fuel cell was maintained at 80 and 100C.

A cyclic current aging test was also performed. Each current aging cycle is composed by 3 current steps (high, medium and low current) that lasted 30 s (figure 1).

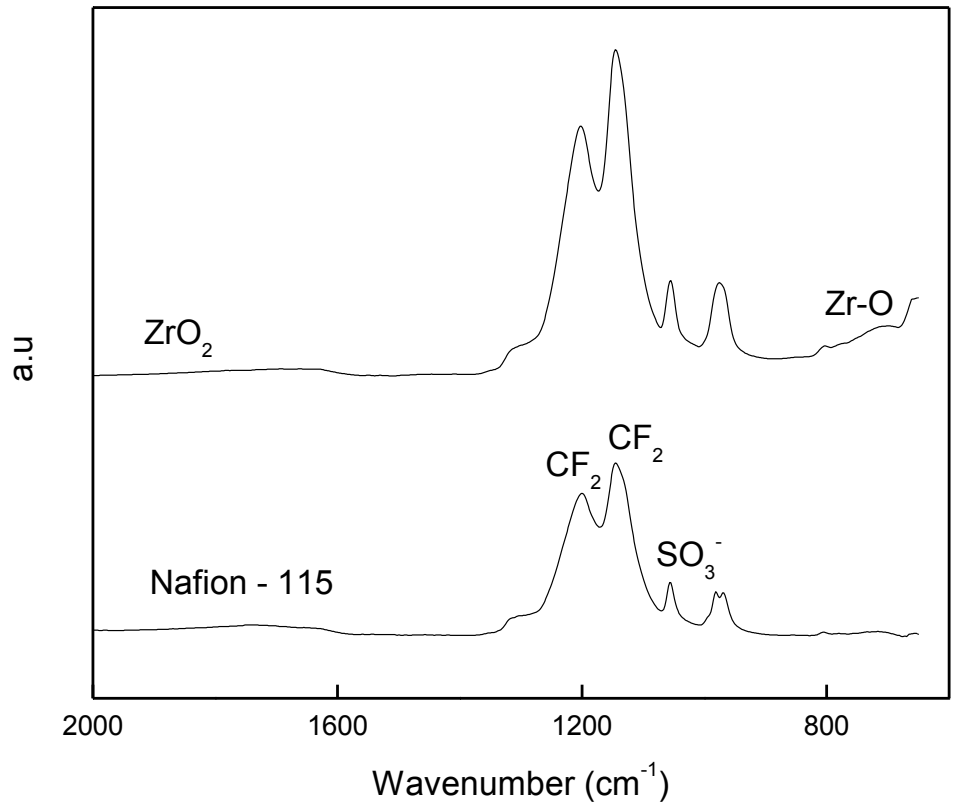

Figure 1. Fourier transforms infrared (FT-IR) spectra of ZrO_2 and Nafion - 115 membranes.

The corresponding responses were registered by recording the voltage as a function of the cycle number. The degradation test was carried at T_{Cell} = 100 C with a back pressure of 30 psi in the anode and the cathode.

3. RESULTS

3.1 Physicochemical properties of composite membranes

Fourier Transform Infrared spectra at wave numbers 4000-400 cm^{-1} for the composite membranes were recorded, analyzed and compared to those obtained for the Nafion 115 membrane. The IR spectrum of the reference and composite membrane are presented in Figure 1. The Nafion - 115 membrane presented two signals at 1199 cm^{-1} and 1146 cm^{-1} that are related to the CF_2 stretching vibration of the PTFE backbone. The peaks observed at 1055 and 967 cm^{-1} are attributed to the stretching vibration moieties of SO_3^- and C-O-C, respectively [33]. The zirconium oxide bands in the composite membrane are observed in the region between 820 – 520 cm^{-1} [26, 34].

The presence ZrO_2 in the composite membrane was also confirmed by SEM/EDX data, shown in Fig. 2. EDX spectra for each membrane indicate elemental peaks for elements carbon, oxygen, fluorine and sulphur. A signal for Zr is observed for the ZrO_2 composite membrane. The EDX mapping images of the composite membrane suggests a homogeneous distribution of Zr.

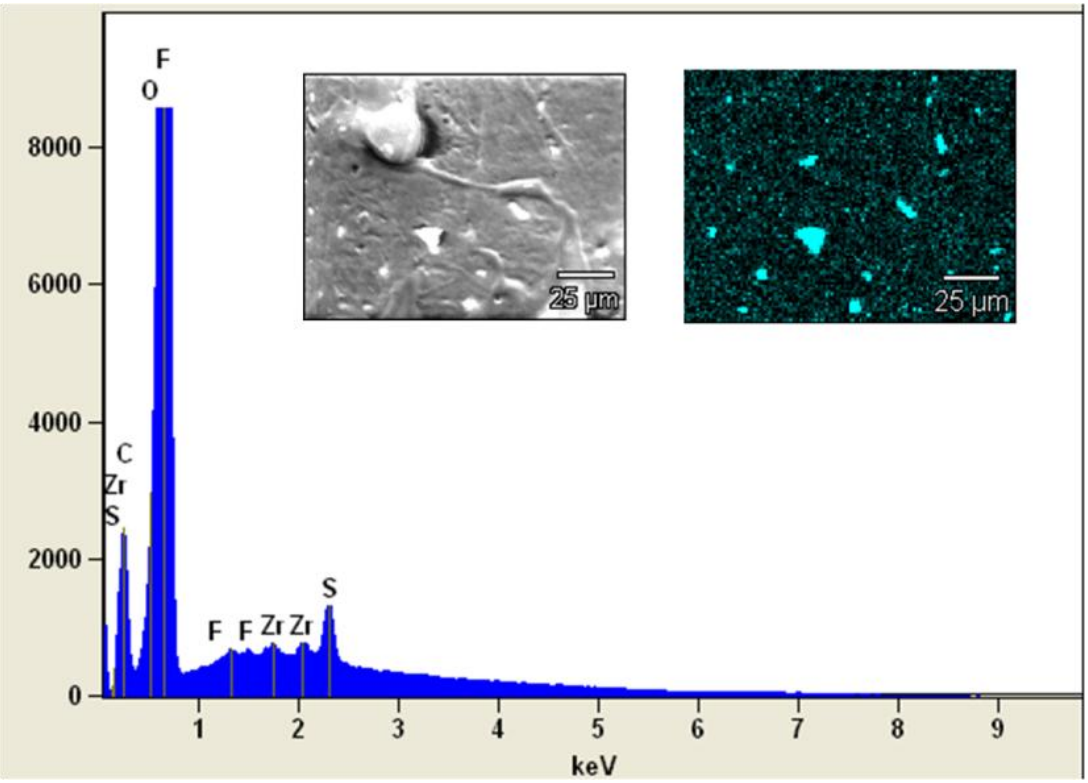

Figure 2. SEM images of composite membrane.

Table 1. Properties Physicochemical of composite membranes

Composite Membrane	WU (%)	IEC (meq/g)	Water molecules per sulfonated group (λ)	Thickness (µm)
Nafion - 115	25.7	1.0093	14.1	127
ZrO2	15	1.076	7.7	59

The water uptake and Ionic Exchange Capacity results of the reference and composite membranes are shown in Table 1. It is interesting to note that the Nafion 115 membrane has a higher water uptake value as compared to that of the composite membrane. In this regard, it is also important to point out that membrane properties may be modified by the casting procedure and the incorporation of the inorganic filler. Ion Exchange capacities of membranes, as measured by titration, reveal that the IEC of the membranes are similar to each other [30].

Figure 3 also shows that the composite membrane has lower methanol permeability (P) than Nafion 115. The methanol permeability (P) of the ZrO_2 membrane corresponds to $1.92X10^{-6}$ cm^2s^{-1} which is lower than that of Nafion 115 ($2.79X10^{-6}$ cm^2s^{-1}) [10] Methanol molecules are easily transferred together with solvated protons, and the number of hydrophilic of groups in Nafion 115 membranes exceeds that of the composite films. I do not understand this sentence!!. The composite membrane has lower methanol permeability (P), because the metal oxide (ZrO_2) blocks the ion-exchange groups (sulfonic groups) in the polymer (Nafion), creating a tortuous path for methanol [32, 35].

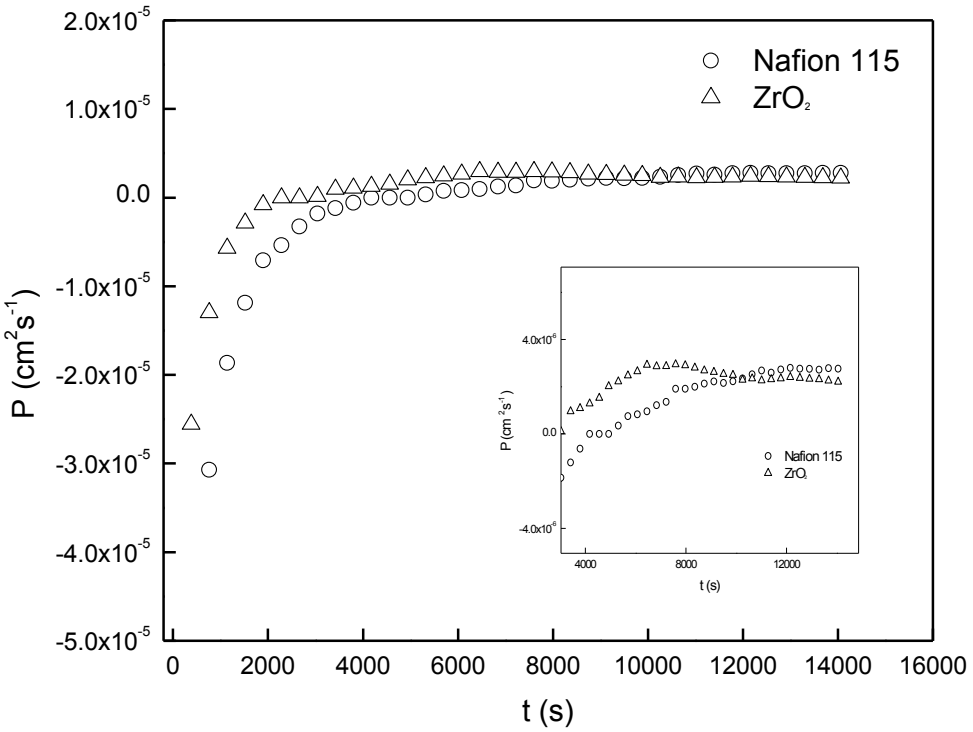

Figure 3. Methanol permeability rate curves of Nafion 115 and ZrO_2 membranes (25 °C).

3.2 Fuel cell Performance

In agreement with the methanol permeation measurements and the expected effect in the methanol crossover behavior, the polarization curves of the composite membranes (see Figure 4), and reveal that the composite membrane shows a better performance than that of the Nafion – 115 at the two temperatures surveyed (80 and 100 C).

At 80 C the fuel cell built with the ZrO_2 modified membrane achieved a maximum power density of 0.067 W cm^{-2} which is roughly six times larger to that obtained for the Nafion – 115 fuel cell (0.013 W cm^{-2}). At higher temperatures (100 C), the Nafion containing fuel cell performance felt down around 30 % (0.009 W cm^{-2}) when compared to the power density obtained at 80C. Contrary to this trend, at this temperature operation conditions, the ZrO_2 membrane improved the performance of the fuel cell about 12 % (0.076 W cm^2).

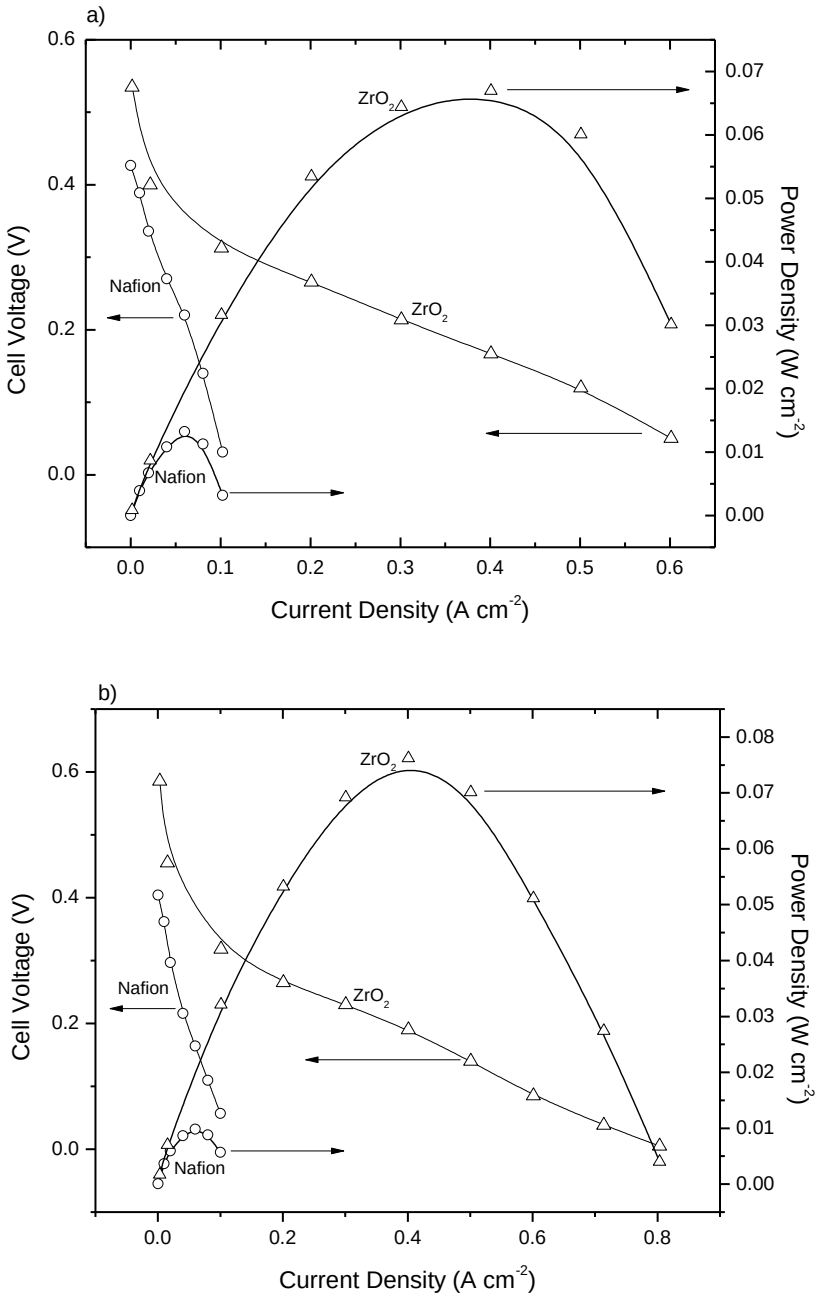

Figure 4. Polarization Curves of Nafion and ZrO_2 membranes at a) 80 and b) 140 °C.

It is also interesting to note that at the two temperatures surveyed, the composite membrane shows a lower value of resistance and open circuit voltage (OCV) when compared to that of Nafion (Table 2). The low OCV and performance values observed for Nafion should be related to the methanol crossover effect.

A current aging cyclic was carried out for the composite and Nafion membrane fuel cell devices. The performance of the commercial membrane (Nafion 115) decreases with the number of cycles (Figure 5 a), resulting in a final power density of 0.003 W cm^{-2}; which is about three times less than that corresponding to its initial value (0.009 W cm^{-2}).

Table 2. Parameters obtained from the composite membrane from the aging cycle.

Membrane	Nafion			ZrO2		
Cycle	R	OCV	WMax	R	OCV	WMax
0	0.292	0.404	0.009	0.131	0.587	0.076
250	0.301	0.391	0.008	0.125	0.587	0.099
500	0.313	0.371	0.006	0.117	0.587	0.12
750	0.417	0.352	0.003	0.232	0.587	0.051
1000	0.431	0.394	0.002	0.128	0.586	0.062
1250	0.426	0.408	0.002	0.116	0.586	0.088

Cell Resistance (R) = Ω cm^2; Open Circuit Voltage (OCV) = V; Power Density (W_{Max}) = Wcm^{-2}

As expected, the internal cell resistance (figure 5 b) increases with the number of cycles due to the methanol permeation that takes place from the anode towards the cathode. For the ZrO_2 composite membrane on the other hand (Figure 5 c), the power density augments as the number of cycles increases, reaching a power density of 0.12 W cm^{-2} and then, after 500 cycles the power density falls to 0.051 W cm^{-2}. Consistent with these results, the cell resistance (Figure 5 d) for the ZrO_2 decreases until 500 cycles is carried out.

In Table 2, the parameters obtained from the aging cycle experiments are shown. The OCV for the Nafion membrane decreases as the number of cycles applied. This behavior is related to the methanol crossover from the anode to the cathode.

In order to determine the CO poisoning on the anode catalyst, a voltammetry analysis was performed to each membrane before and after the aging cycle. In figure 6 the corresponding cyclic voltammetry (CV) are shown. , As can be seen from the corresponding data, the electroactive area is decreased with aging cycles as compared to that observed from the CV at the beginning of the experiment.

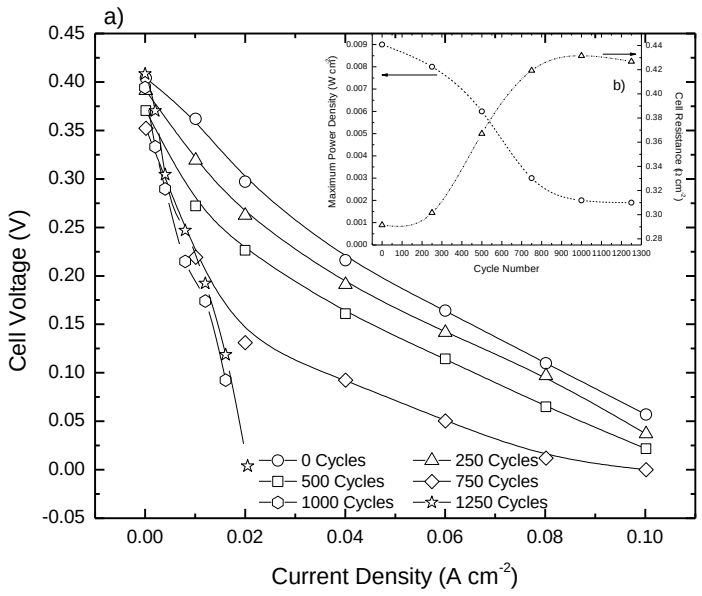

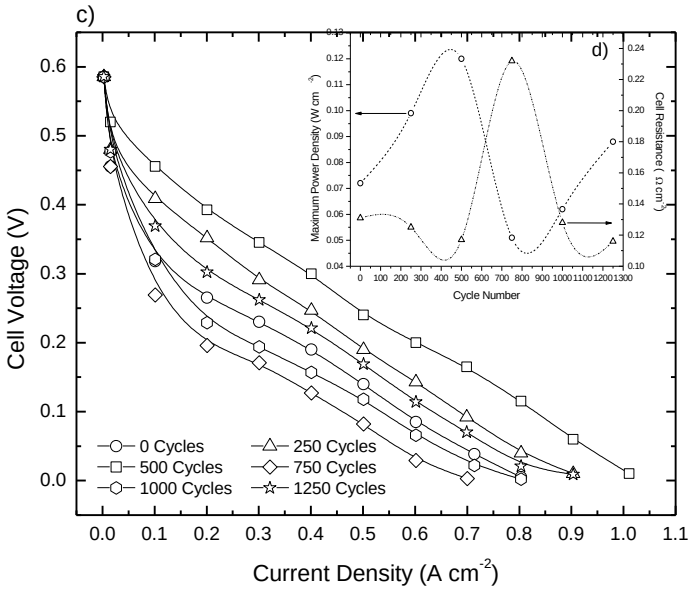

Figure 5. Polarization curves every 250 cycles at T_{cell} = 100 °C for a) Nafion and c) ZrO_2.

The incorporation of the inorganic filler shows that as expected the tendency is the same but the decrease rate with the aging cycles is less severe than that observed for the Nafion membrane. These results can be explained in terms of the different methanol permeation properties of the two membranes under study.

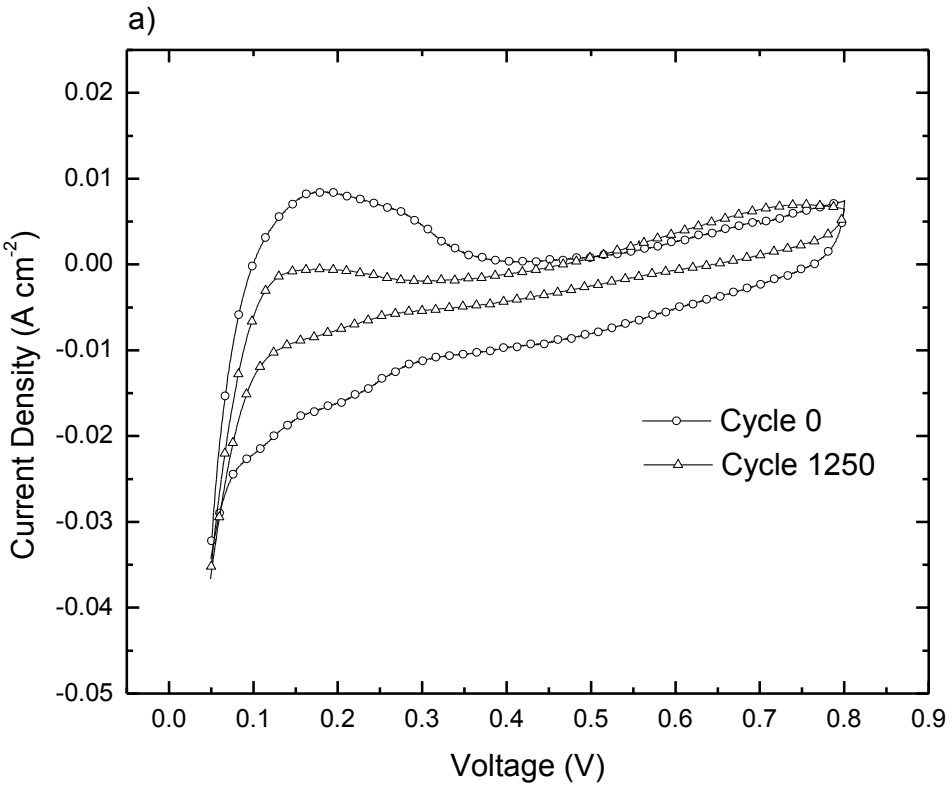

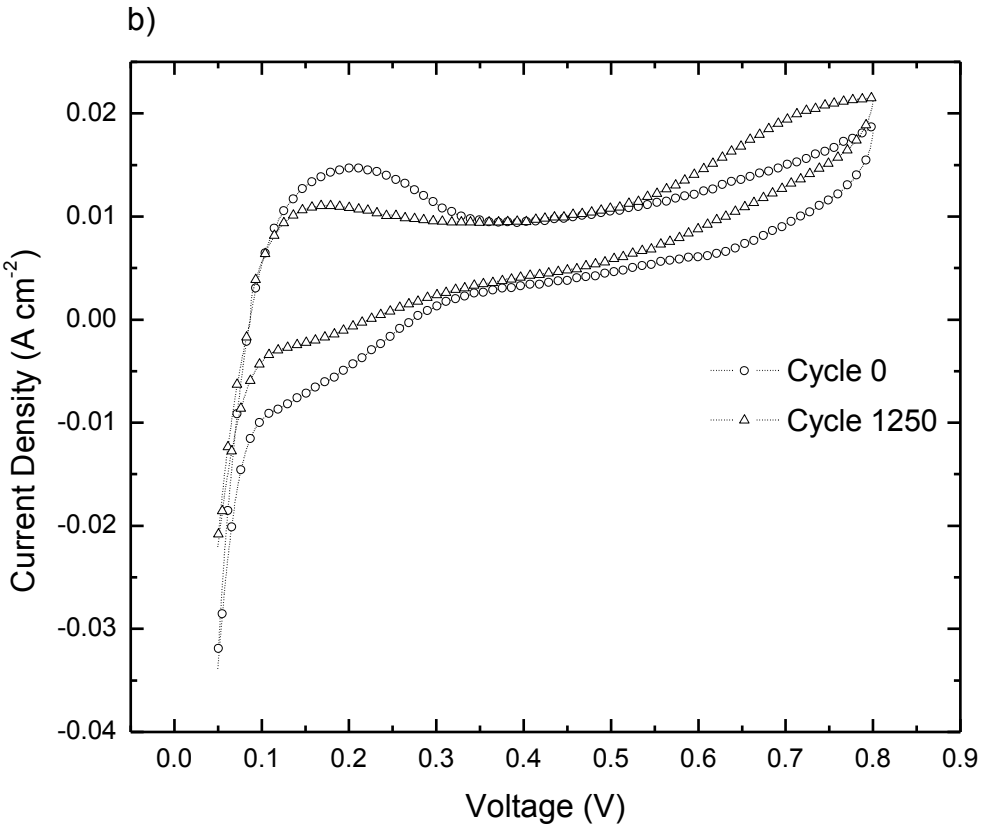

Figure 6. Cyclic voltammetry at the anode for a) Nafion and c) ZrO_2 membranes

4. CONCLUSIONS

This paper presents the characterization and evaluation of the methanol permeation properties of composite membranes prepared from a mixture of Nafion® 5% and 3% wt. of ZrO_2 as filler. The composite membrane based in the inorganic filler showed a significant decrement in the methanol permeation, when compared to the commercial Nafion® 115 membrane. Since methanol diffuses to the cathode and reacts with oxygen to produce carbon monoxide, which easily adsorbs on the Pt active sites, the number of active sites for oxygen reduction decreases. In this context, this phenomenon is suppressed by the inclusion of ZrO_2 fillers because, more active sites for oxygen reduction are protected by the limiting methanol permeation effect of the modifier [14]. In this way, the inorganic filler could be hindering the passage of methanol by blocking exchange groups which reduces the permeation of alcohol and improved the fuel cell performance.

ACKNOWLEDGMENTS
The authors thank the Mexican Council for Science and Technology CONACYT for financial support through SEP-CONACYT 2009-133310 and Fomix-Chihuahua 127461.

References

1. A. Casalegno, P. Grassini, R. Marchesi, *Applied Thermal Engineering*, 27 (2007) 748-754.

2. E. Kjeang, J. Goldak, M.R. Golriz, J. Gu, D. James, K. Kordesch, *J. Power Sources*, 153 (2006) 89-99.
3. J.-Y. Park, J.-H. Lee, S. Kang, J.-H. Sauk, I. Song, *J. Power Sources*, 178 (2008) 181-187.
4. X. Li, E.P.L. Roberts, S.M. Holmes, *J. Power Sources*, 154 (2006) 115-123.
5. V.B. Oliveira, C.M. Rangel, A.M.F.R. Pinto, *Int. J. Hydrogen Energy*, 34 (2009) 8245-8256.
6. V.S. Silva, J. Schirmer, R. Reissner, B. Ruffmann, H. Silva, A. Mendes, L.M. Madeira, S.P. Nunes, *J. Power Sources*, 140 (2005) 41-49.
7. V.B. Oliveira, C.M. Rangel, A.M.F.R. Pinto, *Int. J. Hydrogen Energy*, 34 (2009) 6443 – 6451.
8. H. Ahmad, S.K. Kamarudin, U.A. Hasran, W.R.W. Daud, *Int. J. Hydrogen Energy*, 35 2160-2175.
9. A.-C. Dupuis, *Progress in Materials Science*, In Press, Corrected Proof.
10. A. Küver, K. Potje-Kamloth, *Electrochim. Acta*, 43 (1998) 2527-2535.
11. S.J. Peighambardoust, S. Rowshanzamir, M. Amjadi, *Int. J. Hydrogen Energy*, 35 9349-9384.
12. A.S. Arico, V. Baglio, A.D. Blasi, V. Antonucci, *Electrochem. Commun.*, 5 (2003) 862-866.
13. A.S. Aricò, V. Baglio, A. Di Blasi, P. Creti, P.L. Antonucci, V. Antonucci, *Solid State Ionics*, 161 (2003) 251-265.
14. H. Hou, G. Sun, Z. Wu, W. Jin, Q. Xin, *Int. J. Hydrogen Energy*, 33 (2008) 3402-3409.
15. M.K. Mistry, N.R. Choudhury, N.K. Dutta, R. Knott, Z. Shi, S. Holdcroft, *Chem. Mater.*, 20 (2008) 6857-6870.
16. K.T. Adjemian, S.J. Lee, S. Srinivasan, J. Benziger, A.B. Bocarsly, *J. Electrochem. Soc.*, 149 (2002) A256-A261.
17. R.K.A.M. Mallant, *J. Power Sources*, 118 (2003) 424-429.
18. Y. Shao, G. Yin, Z. Wang, Y. Gao, *J. Power Sources*, 167 (2007) 235-242.
19. J. Pan, H. Zhang, W. Chen, M. Pan, *Int. J. Hydrogen Energy*, 35 2796-2801.
20. D.H. Aguilar, L.C. Torres-González, L.M. Torres-Martínez, T. López, P. Quintana, *Ciencia UANL*, 6 (2003) No. 1.
21. J. González-Hernández, J.F.P. Robles, J.R.M. F. Ruiz, *Superficies y Vacío*, 11 (2000) 1 - 16.
22. S. Melada, M. Signoretto, S.A. Ardizzone, C.L. Bianchi, *Catalysis Letters*, 75 (2001) 199-204.
23. A. Morales-Acevedo, G.F. Pérez-Sánchez, *Superficies y Vacío*, 16 (2003) 16-18.
24. R. Pérez-Hernández, J. Arenas-Alatorre, D. Mendoza-Anaya, A. Gómez-Cortés, G. Díaz, *Revista Mexicana de Física* 50 (2004) 80-84.
25. M.L. Rojas -Cervantes, R.M. Martin -Aranda, A.J. Lopez -Peinado, J.D.D. Lopez -Gonzalez, *J. Materi. Sci.*, 29 (1994) 3743-3748.
26. V. Santos, M. Zeni, C.P. Bergmann, J.M. Hohemberger, *Rev. Adv. Mater. Sci*, 17 (2008) 62-70.
27. A. Saccà, A. Carbone, E. Passalacqua, A. D´Epifanio, S. Licoccia, E. Traversa, E. Sala, F. Traini, R. Ornelas, *J. Power Sources*, 152 (2005) 16 - 21.
28. A. Saccà, A. Carbone, R. Pedicini, G. Portable, L. D´Ilario, A. Longo, A. Martorana, E. Passalacqua, *J. Membrane Sci.*, 278 (2006) 105 - 113.
29. A. Saccà, I.G.A. Carbone, R. Pedicini, E. Passalacqua, *J. Power Sources*, 163 (2006) 47
30. A. Carbone, R. Pedicini, A. Saccà, I. Gatto, E. Passalacqua, *J. Power Sources*, 178 (2008) 661 - 666.
31. M.P. Rodgers, Z. Shi, S. Holdcroft, *J. Membrane Sci.*, 325 (2008) 346-356.
32. T. Li, Y. Yang, *J. Power Sources*, 187 (2009) 332 - 340.
33. V. Di Noto, R. Gliubizzi, E. Negro, G. Pace, *J. Phys. Chem. B*, 110 (2006) 24972-24986.
34. L.A. Cortez-Lajas, J.M. Hernández-Enríquez, A. Castillo-Mares, J.L. Rivera-Armenta, G. Sandoval-Robles, L.A. García-Serrano, R. García-Alamilla, *Revista Mexicana de Ingeniería Química*, 5 (2006) 321 - 327.
35. Y.-F. Lin, C.-Y. Yen, C.-C.M. Ma, S.-H. Liao, C.-H. Lee, Y.-H. Hsiao, H.-P. Lin, *J. Power Sources*, 171 (2007) 388 - 395.